Université de Strasbourg

Institut Terre & Environnement de Strasbourg | ITES | UMR 7063 de l'Université de Strasbourg & cnrs & ENGEES

Influence of wettability on water-air relative permeability curves in unconsolidated porous media: from water-wet to oil-wet

Kevin Hernandez-Perez[a], Gerhard Schäfer[a], Amir H. Alizadeh[b], Mohammad Piri[b], Renaud Toussaint[a,c]

[a]Institut Terre et Environnement de Strasbourg (ITES) UMR 7063, Université de Strasbourg, CNRS, Strasbourg, France.

[b] Center of Innovation for Flow through Porous Media (COIFPM), Department of Energy and Petroleum Engineering, University of Wyoming, Laramie, Wyoming, USA.

[c] PoreLab, The Njord Centre, Department of Physics, University of Oslo, Oslo, Norway

Materials and methods: the porous media

- Two types of quartz sands, P100 and P2040, were used.
- P100 is classified as a fine sand, whereas P2040 is classified as a medium sand.

Learn more

Gerhard Schäfer, Kevin Hernandez Perez, Panav Hulsurkar, Magda Ibrahim Youssif, François Lehmann, Mohammad Piri, Influence of wettability on water retention curves in unconsolidated porous media, Journal of Contaminant Hydrology, Volume 269, 2025.

	P2040	P2040ag	P100	P100ag
oil-water θ_{ow} (°)	39.0±8.8	98.5±12.9	35.8±5.2	93.3±9.4
gas-oil θ_{go} (°)	47.0±6.0	26.4±4.2	45.3±6.2	27.5±4.7
gas-water θ_{gw} (°)	24.1±5.7	46.7±6.4	28.2±6.2	48.8±5.5

Table 1. In situ static contact angles quantified for the four aged and unaged sands (ag=aged)

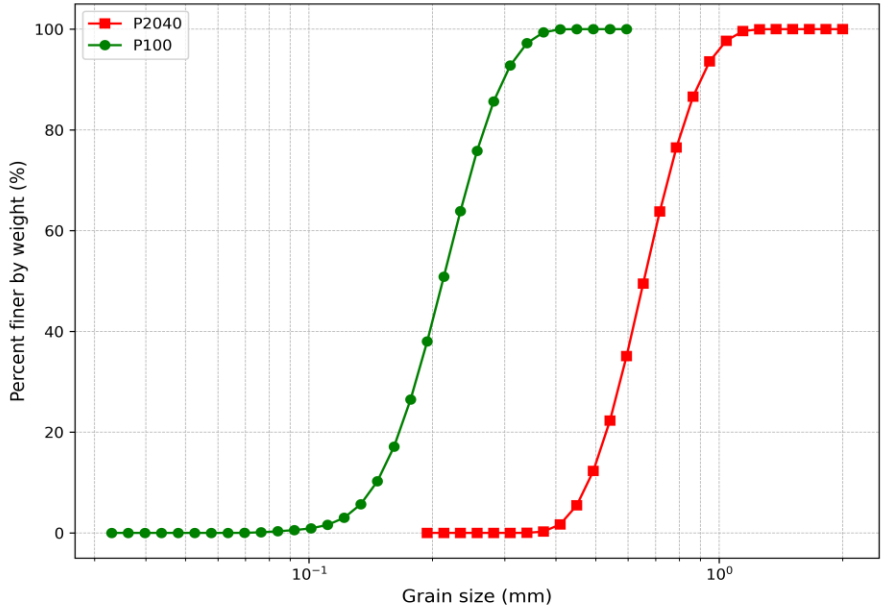

Fig. 1 Cumulative particle size distribution of the experimental porous medium (Schäfer et al., 2025).

Materials and methods: Experimental setup for the measurement of hydraulic conductivity (K_w–S)

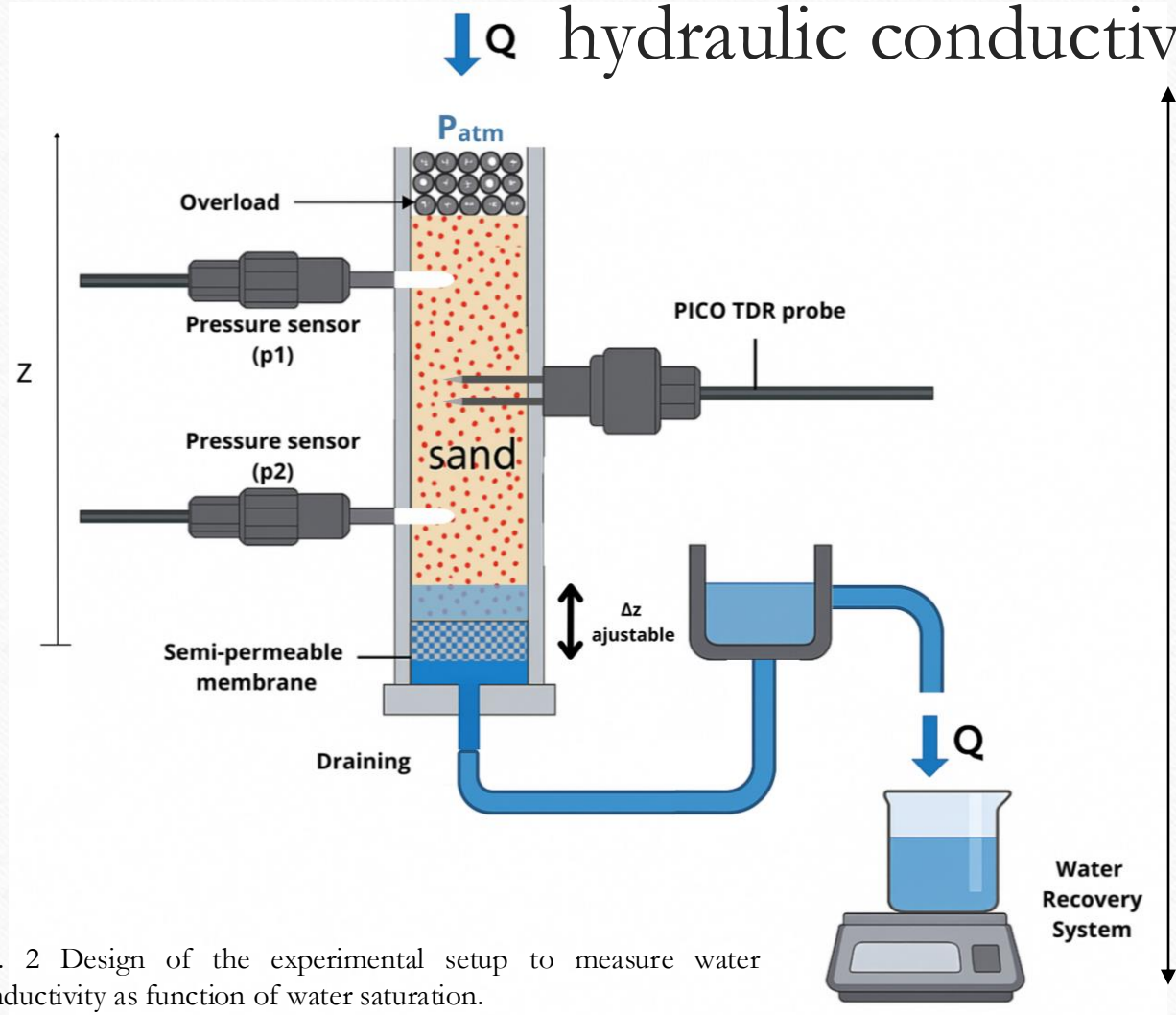

Fig. 2 Design of the experimental setup to measure water conductivity as function of water saturation.

Learn more

Kevin Hernandez-Perez; Gerhard Schäfer; François Lehmann; Mohammad Piri; Renaud Toussaint. An innovative experimental device to quantify the water relative permeability and in situ water retention curves of unconsolidated porous media. Comptes Rendus. Géoscience, Volume 357 (2025)

$$K_w = \frac{Q * L}{S * \left(\Delta z + \frac{\Delta p}{\rho * g}\right)}$$

$$k_{rw}(S_w) = \frac{K_w(S_w)}{K_w(S_{w,mp})}$$

Relative permeability results (k_r)

a) k_{rw} (water-wet sands)

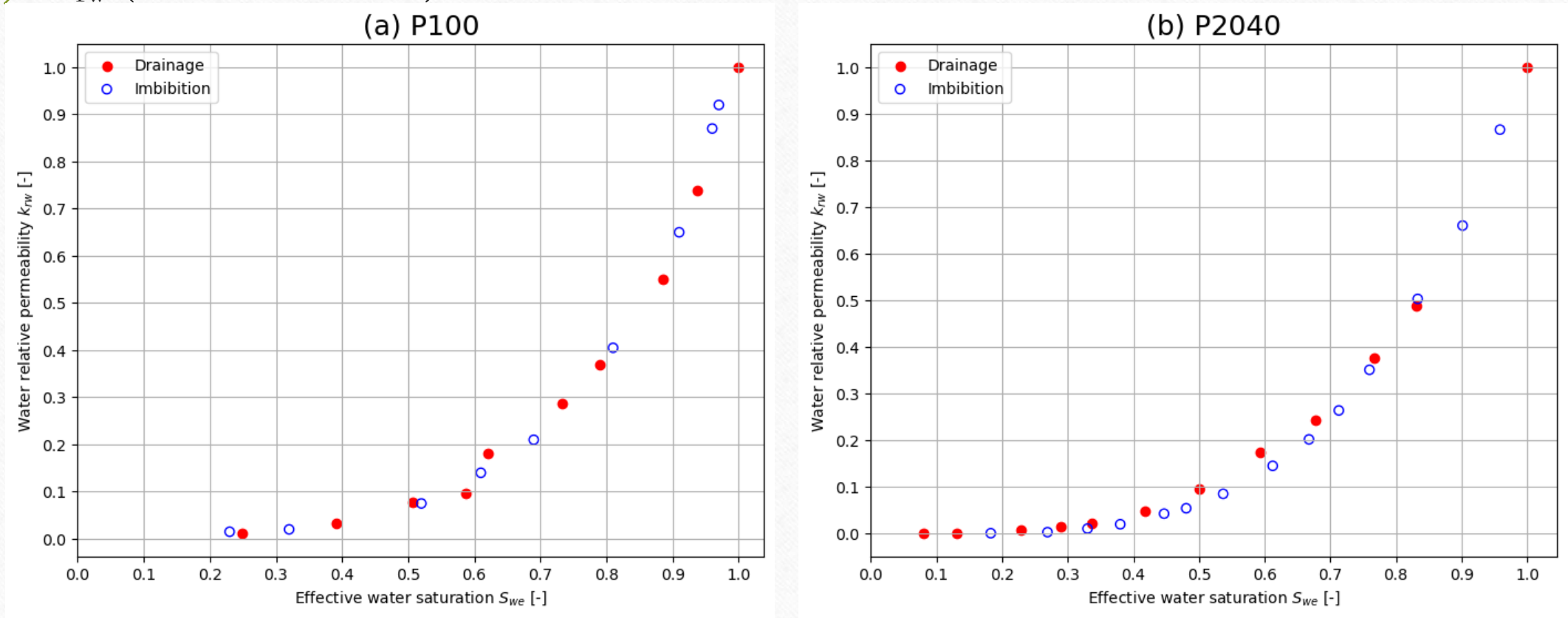

Fig. 3 Experimental water relative permeability (krw) curves as a function of effective water saturation (Swe) for (a) P100 and (b) P2040 sands.

- Minimal hysteresis
- Quasi-unique k_{rw}-S function

$$S_{we} = \frac{S_w - S_{wi}}{S_{w,max} - S_{wi}}$$

b) k_{rw} (oil-wet sands)

- Hysteresis presence

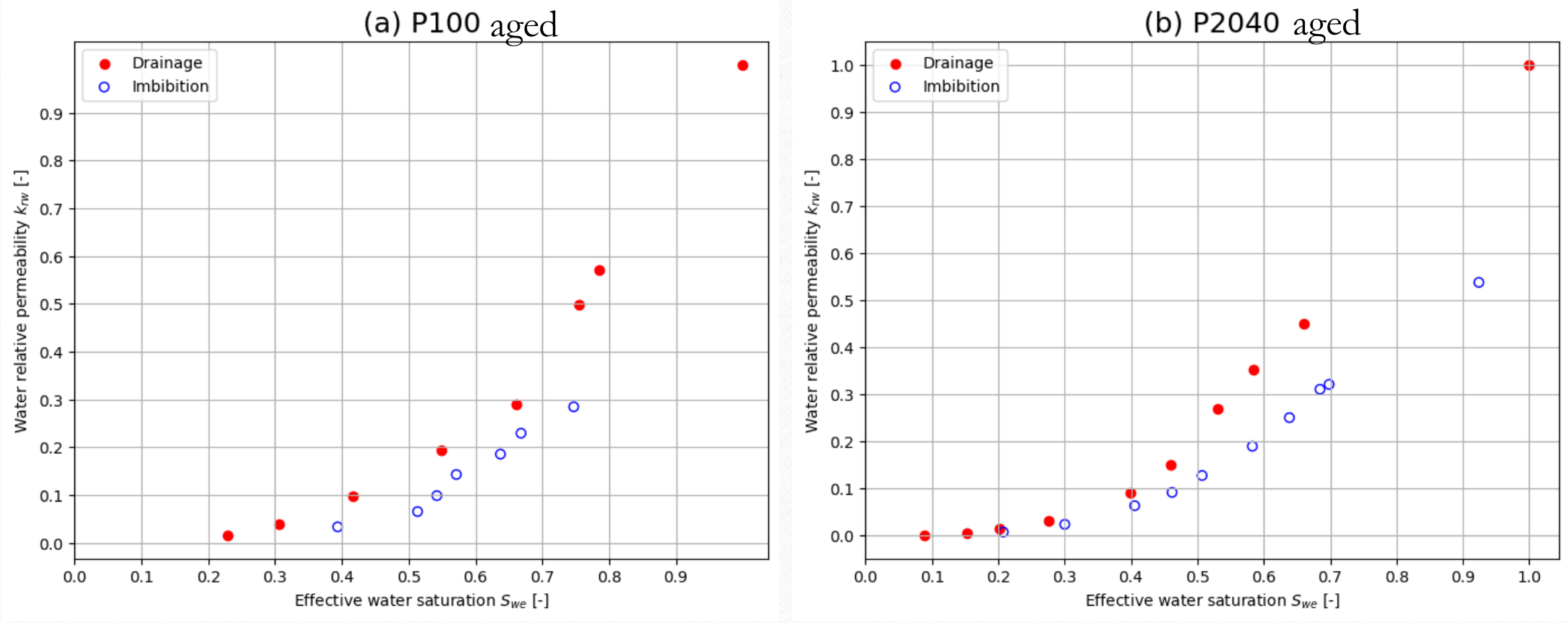

Fig. 4 Experimental water relative permeability (krw) curves as a function of effective water saturation (Swe) for the (a)P100 and (b)P2040 sands under oil-wet conditions.

c) k_{rw} (fractional wetting) (50% water-wet, 50% oil-wet)

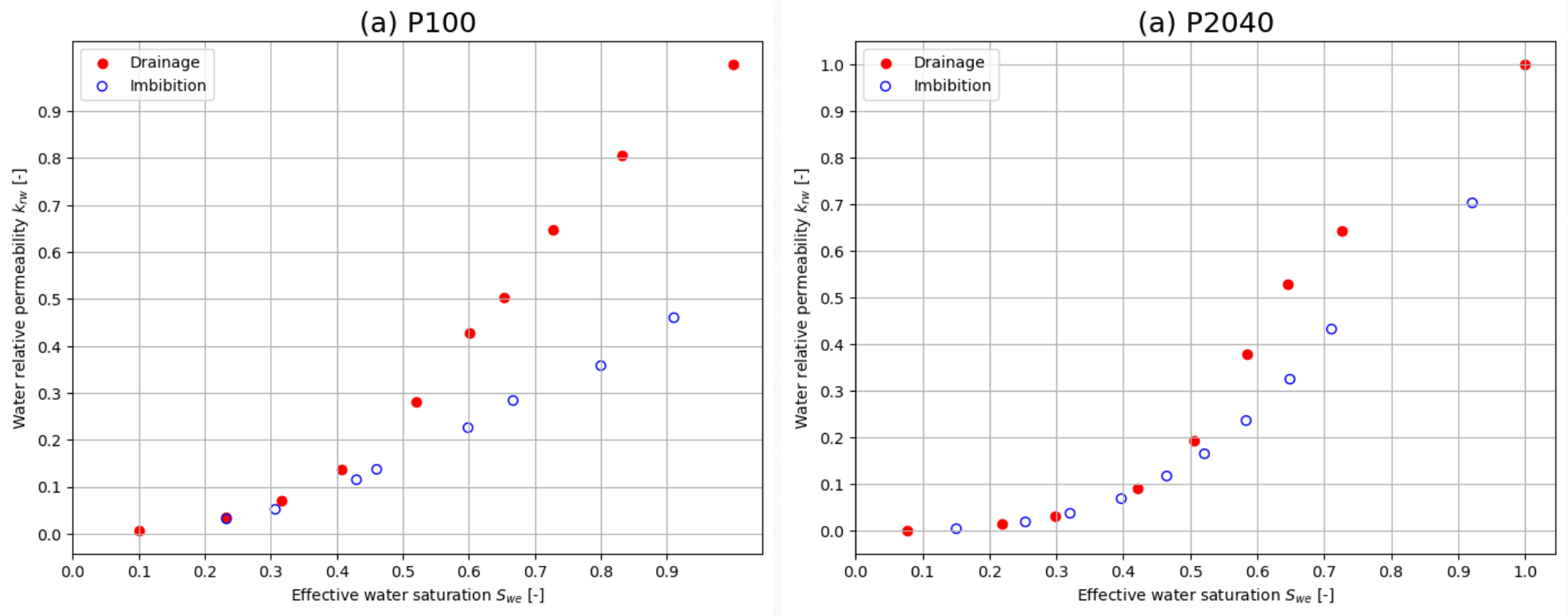

Fig. 5 Water relative permeability (krw) curves as a function of effective water saturation (Swe) for a 50/50 mixture of water-wet and oil-wet sands.

Materials and methods: Experimental setup for the measurement of K_a–S

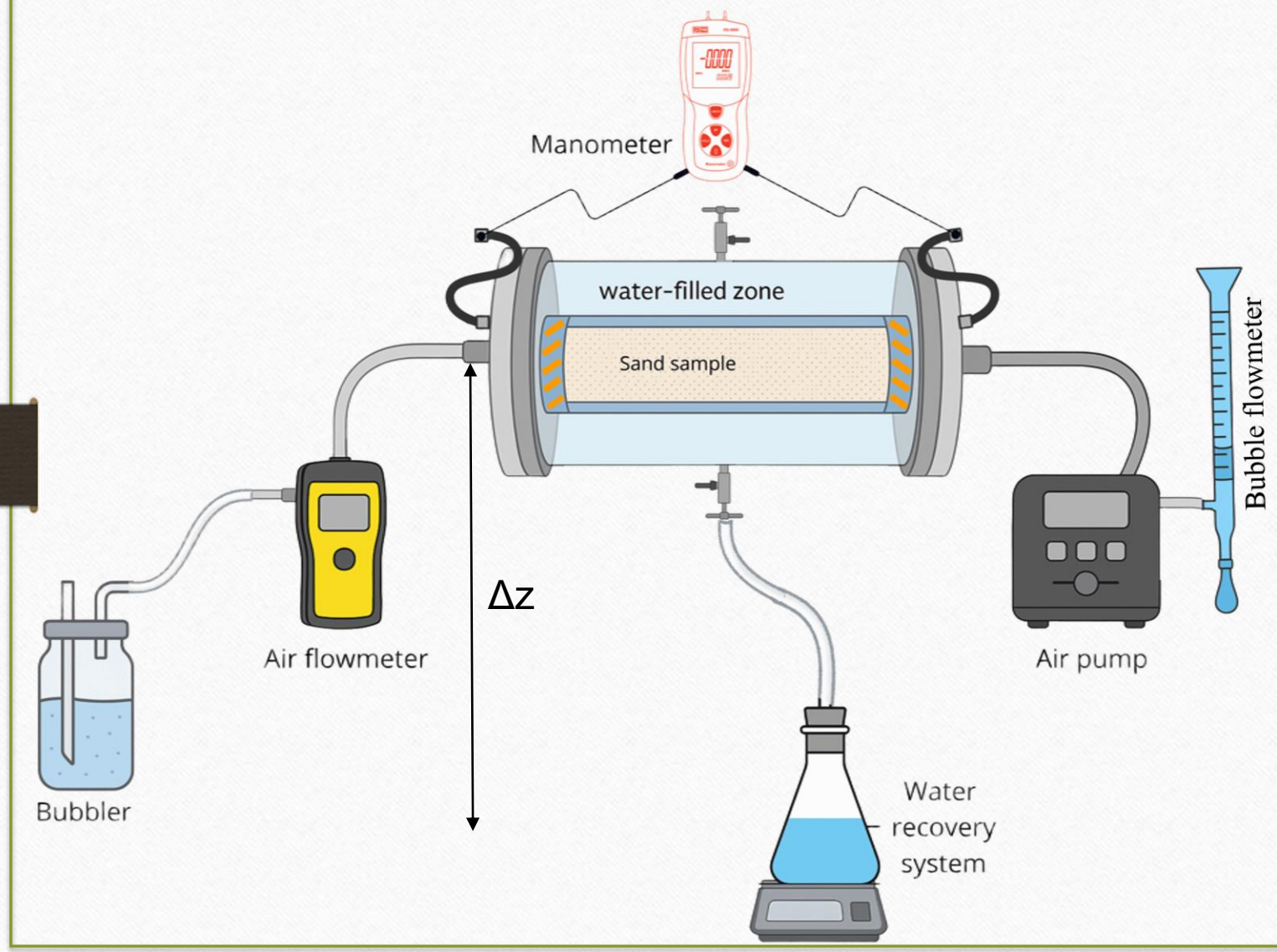

Learn more

Kevin HERNANDEZ-PEREZ, Gerhard SCHÄFER, Amir H. Alizadeh et al. Design of a hydraulically confined column device for simultaneous measurement of air relative permeability and water retention in unconsolidated porous media, 28 April 2026, PREPRINT (Version 1)

$$Q = \frac{S}{\rho_a g} \frac{K_{a,m} \cdot K_{a,s}}{LK_{a,m} + 2eK_{a,s}} \cdot \Delta p$$

$$k_{ra} = \frac{K_{a,s}}{K_{a,mp}}$$

7

Fig. 6 Design of the experimental setup to measure air conductivity as function of water saturation.

Results-k_r

a) k_{ra} (water-wet sands)

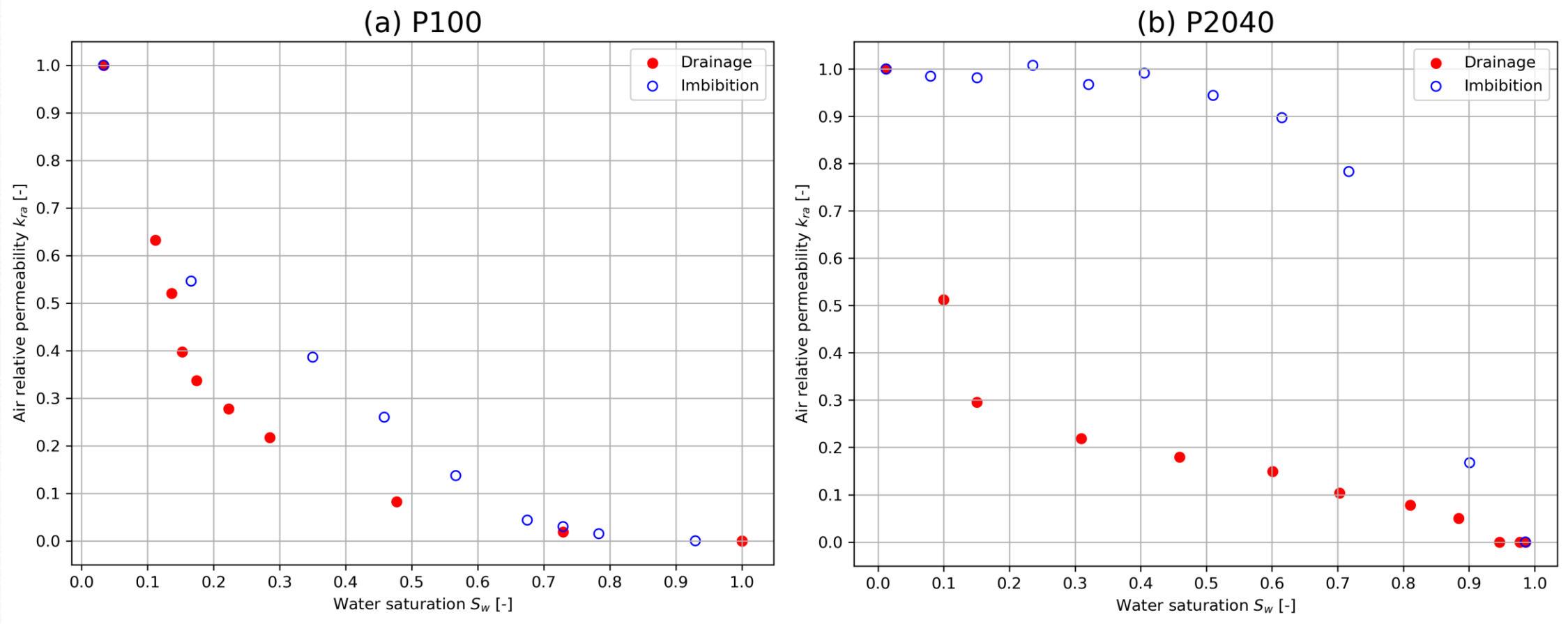

Fig. 7 Experimental air relative permeability (kra) curves as a function of water saturation (Sw) for (a) P100 and (b) P2040 sands.

- Hysteresis presence

b) k_{rw} (oil-wet sands)

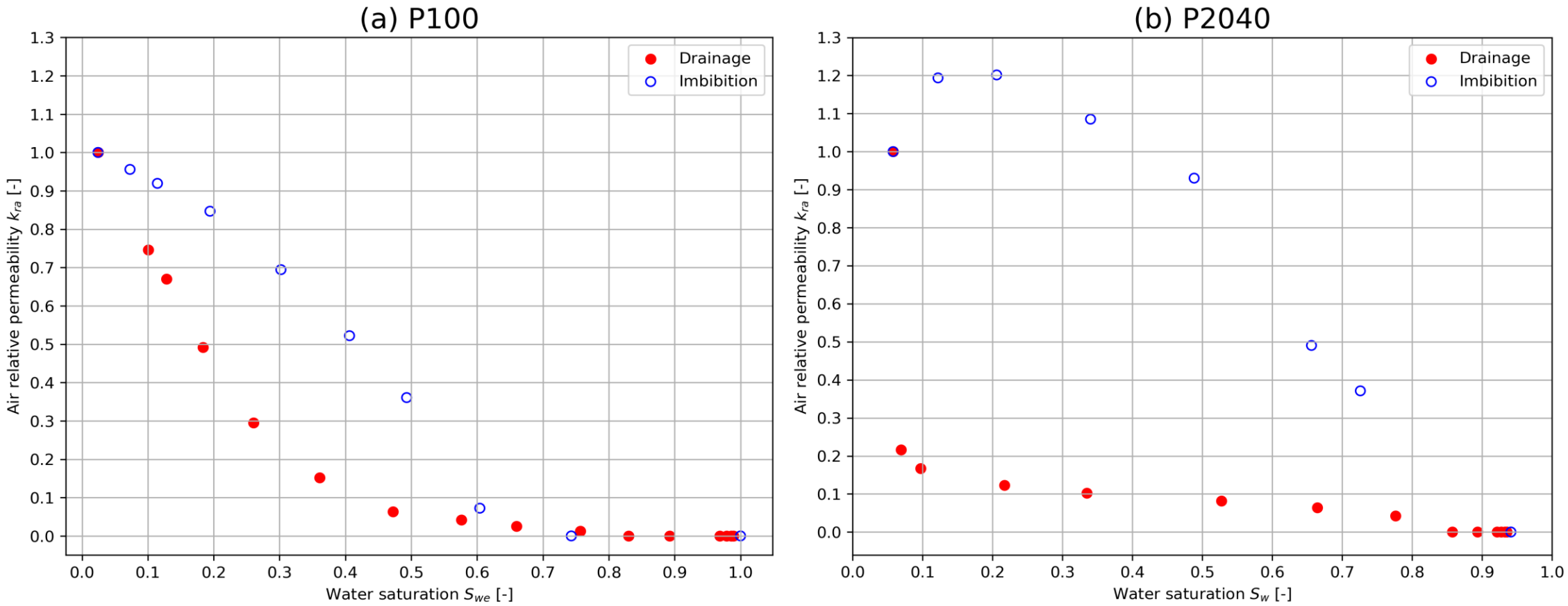

Fig. 8 Experimental air relative permeability (kra) curves as a function of water saturation (Sw) for the (a)P100 and (b)P2040 sands under oil-wet conditions.

- Hysteresis presence
- Viscous coupling

$$q_a = -\frac{k k_{ra}}{\mu_a} \nabla P_a \quad \Rightarrow \quad q_a = -\frac{k}{\mu_a} (k_{aa} \nabla P_a + k_{aw} \nabla P_w)$$

c) k_{ra} (fractional wetting) (50% water-wet, 50% oil-wet)

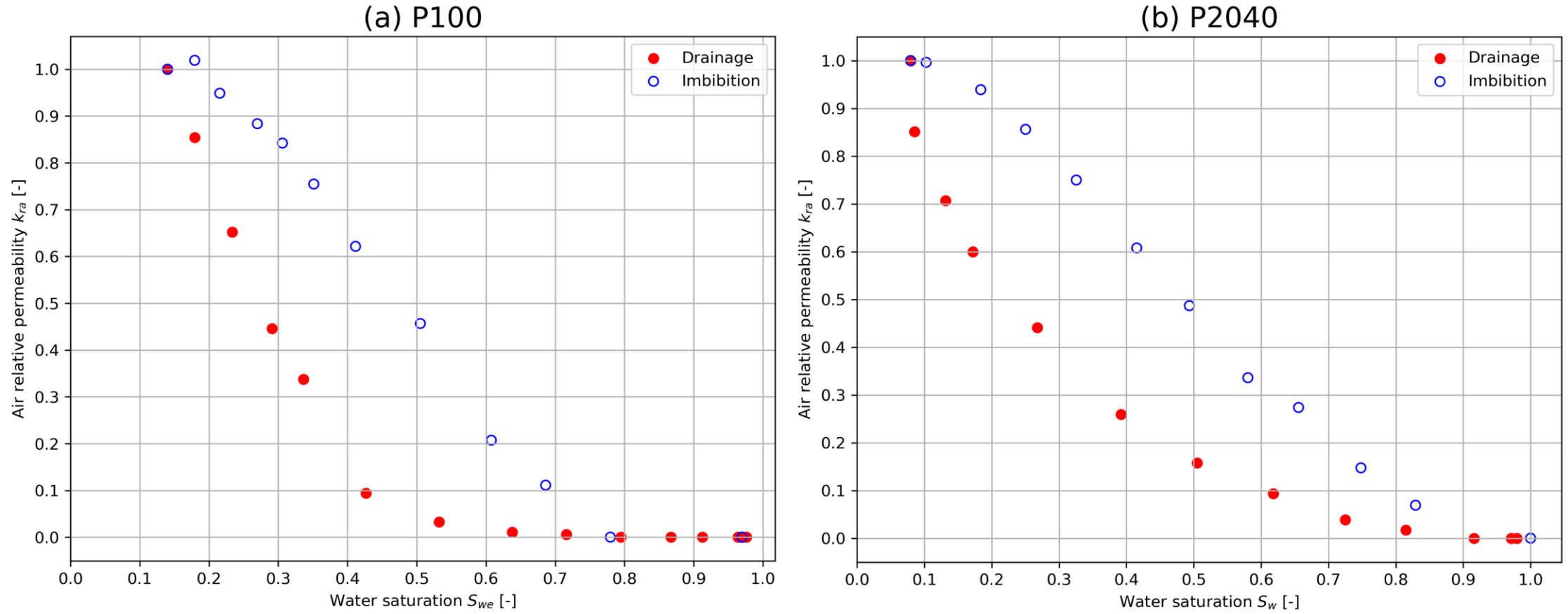

Fig. 9 Experimental air relative permeability (kra) curves as function of water saturation (Sw) for a 50/50 mixture of water-wet and oil-wet sands.

Capillary pressure results (P_c - unaged sands)

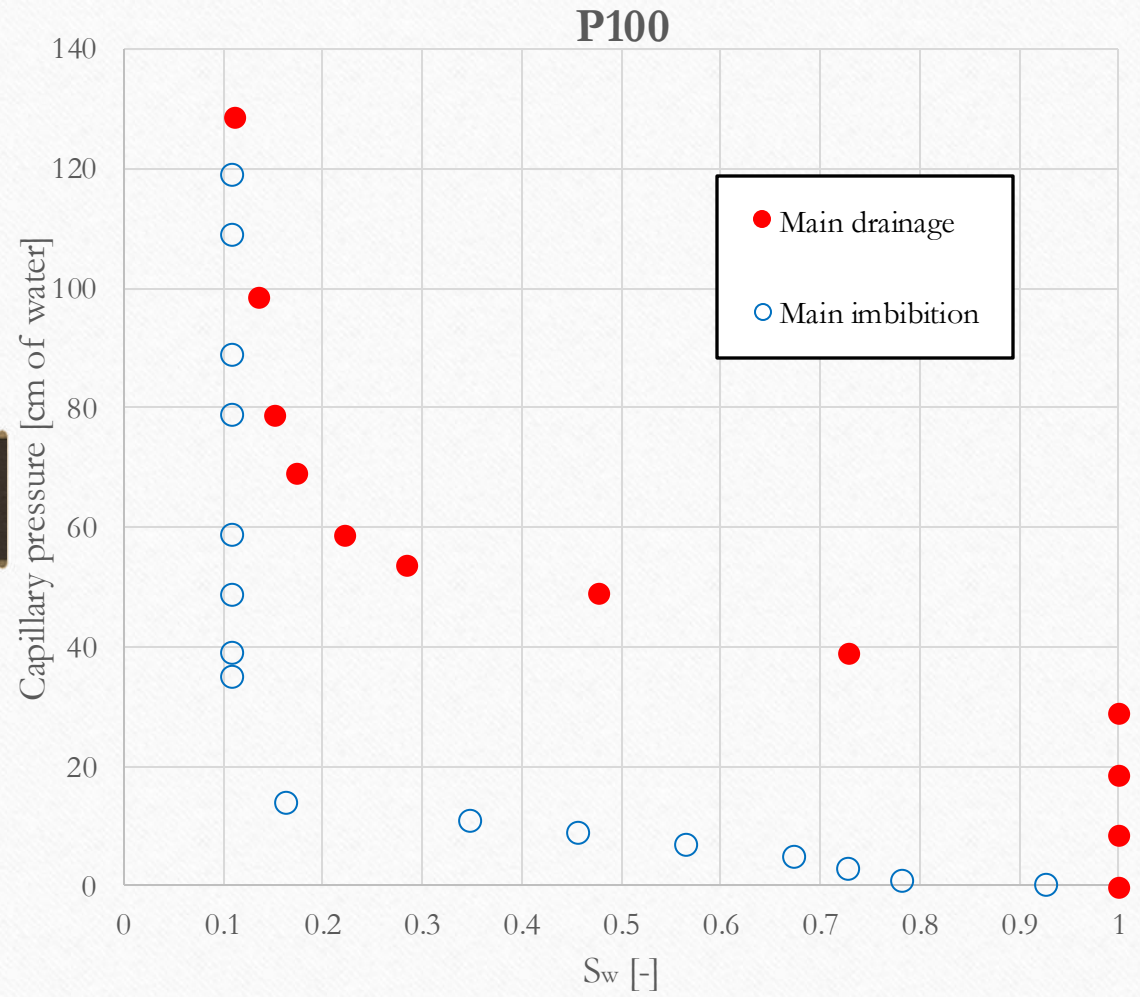

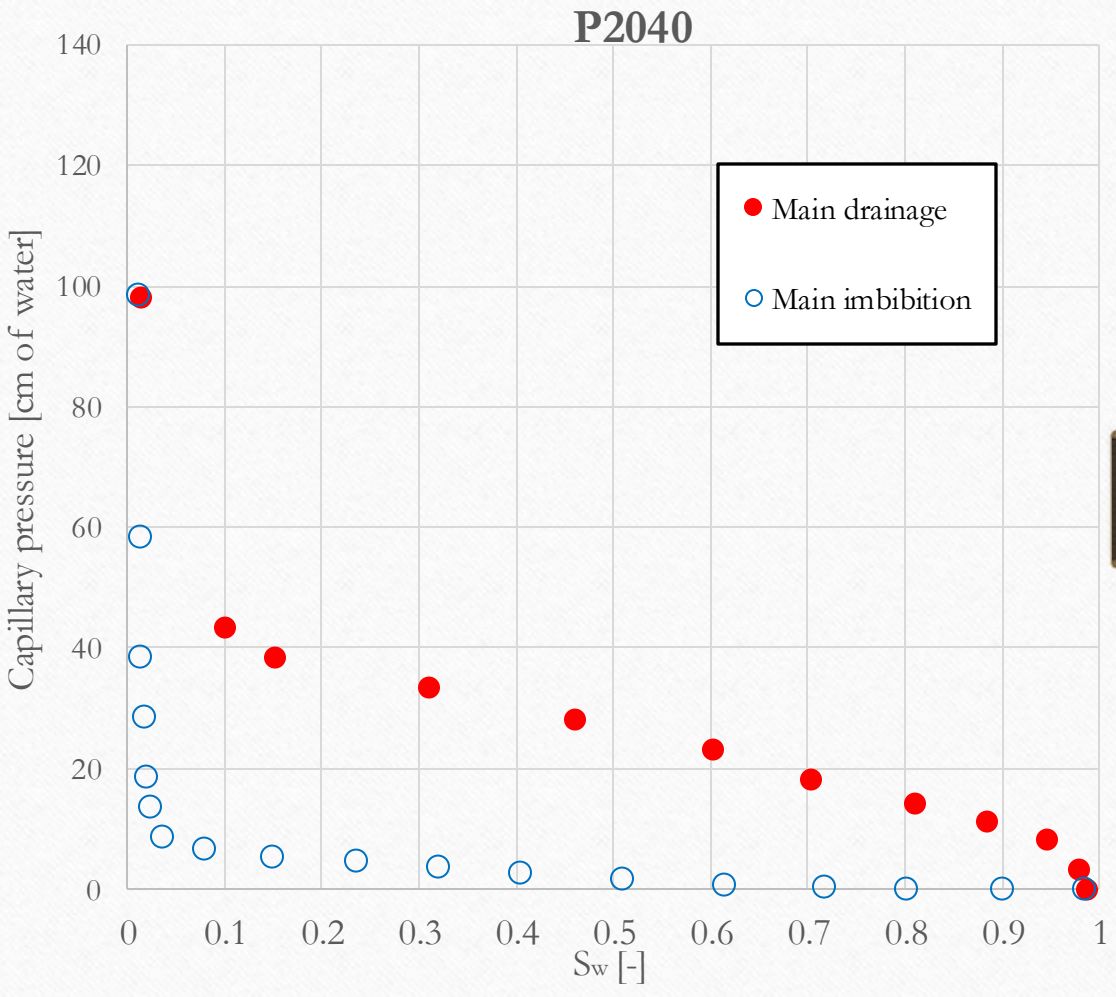

Fig. 10 Experimental water retention curves (Pc) as a function of water saturation (Sw) for the (a) P100 and (b)P2040 sands under water-wet conditions.

Results-Pc (aged sand)

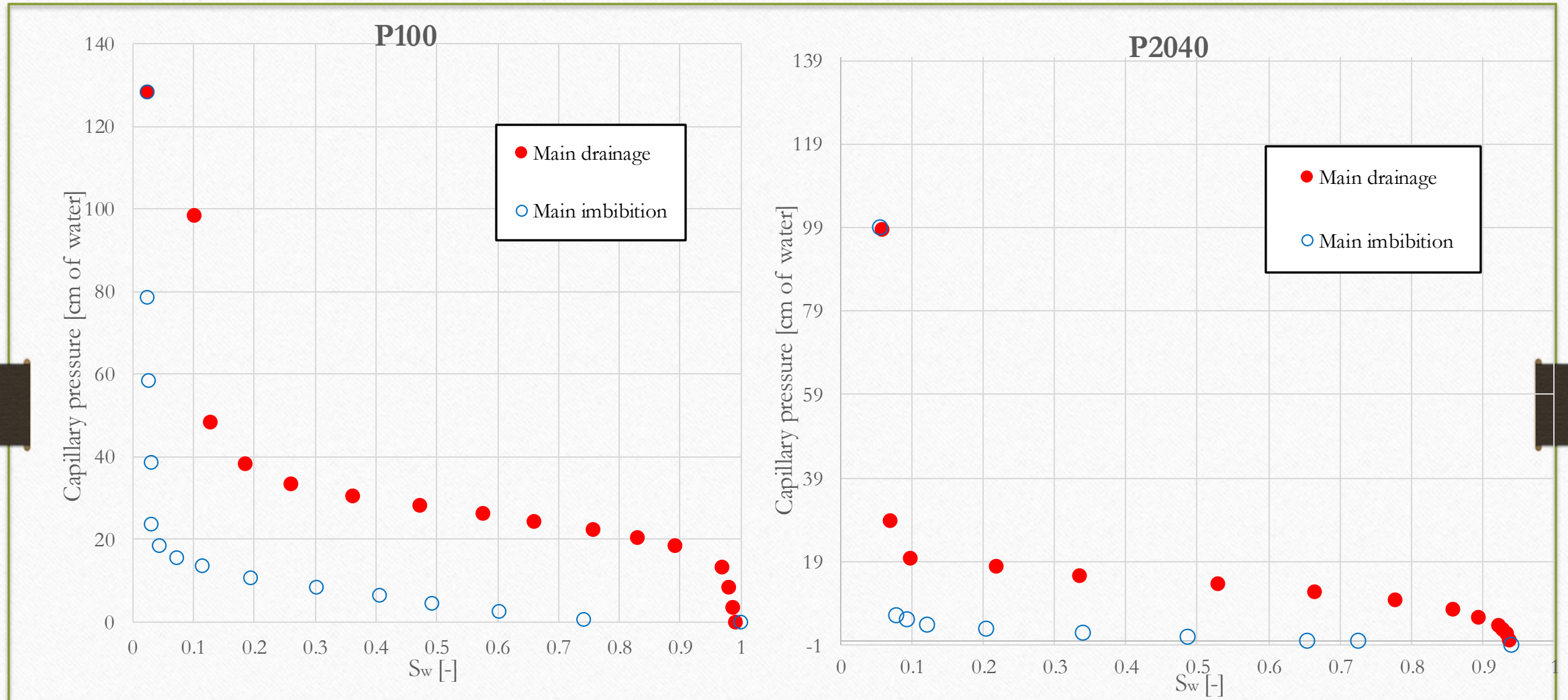

Fig. 11 Experimental water retention curves (Pc) as a function of water saturation (Sw) for the (a) P100 and (b)P2040 sands under oil-wet conditions.

$$S_{we} = \{1 + \ln[1 + (\alpha p_c)^n]\}^{-m}$$

$$m = 1 - \frac{1}{n}$$

Predictive modelling using General van Genuchten (GVG) parameters from water retention curves

(Ghorbani, A., Sadeghi, M., Tuller, M., Durner, W., & Jones, S. B. (2024). A generalized van Genuchten model for unsaturated soil hydraulic conductivity. *Vadose Zone Journal*, *23*(5), e20369. https://doi.org/10.1002/vzj2.20369)

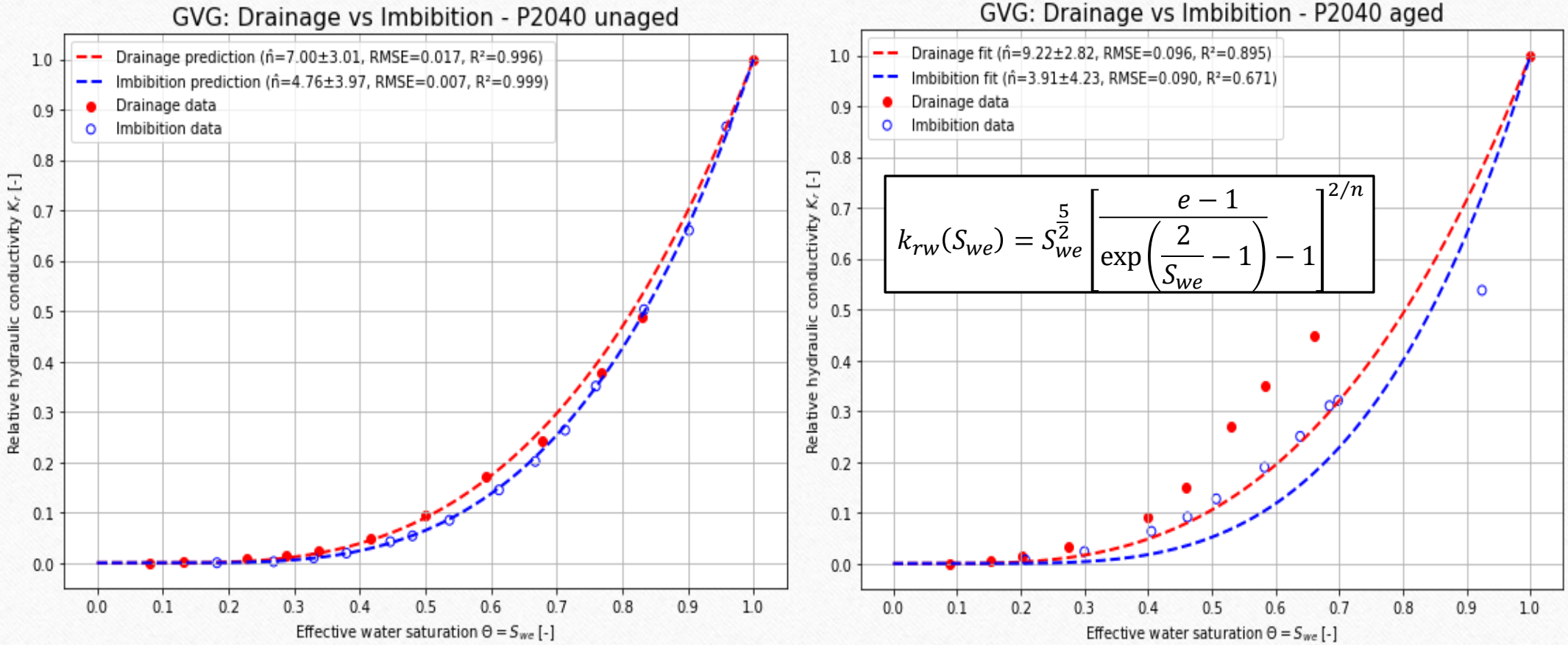

Fig. 12 Water relative permeability (krw) as function of effective water saturation (Swe) for sand P2040. Experimental data are shown for drainage (red filled circles) and imbibition (blue unfilled circles). Solid lines represent the predicted krw curves obtained from the General van Genuchten model using the fitted capillary pressure parameters obtained in Figures 3 and 4.

Predictive modelling using van Genuchten (VG) parameters from water retention curves

$$S_w = \{1 + (\alpha p_c)^n\}^{-m}$$

$$m = 1 - \frac{1}{n}$$

$$K_{ra}(S_w) = \left(\frac{S_{w,max} - S_w}{S_{w,e} - S_{wi}}\right)^{1/2} \left[1 - \left(\frac{S_w - S_{wi}}{S_{w,e} - S_{wi}}\right)^{1/m}\right]^{2m}$$

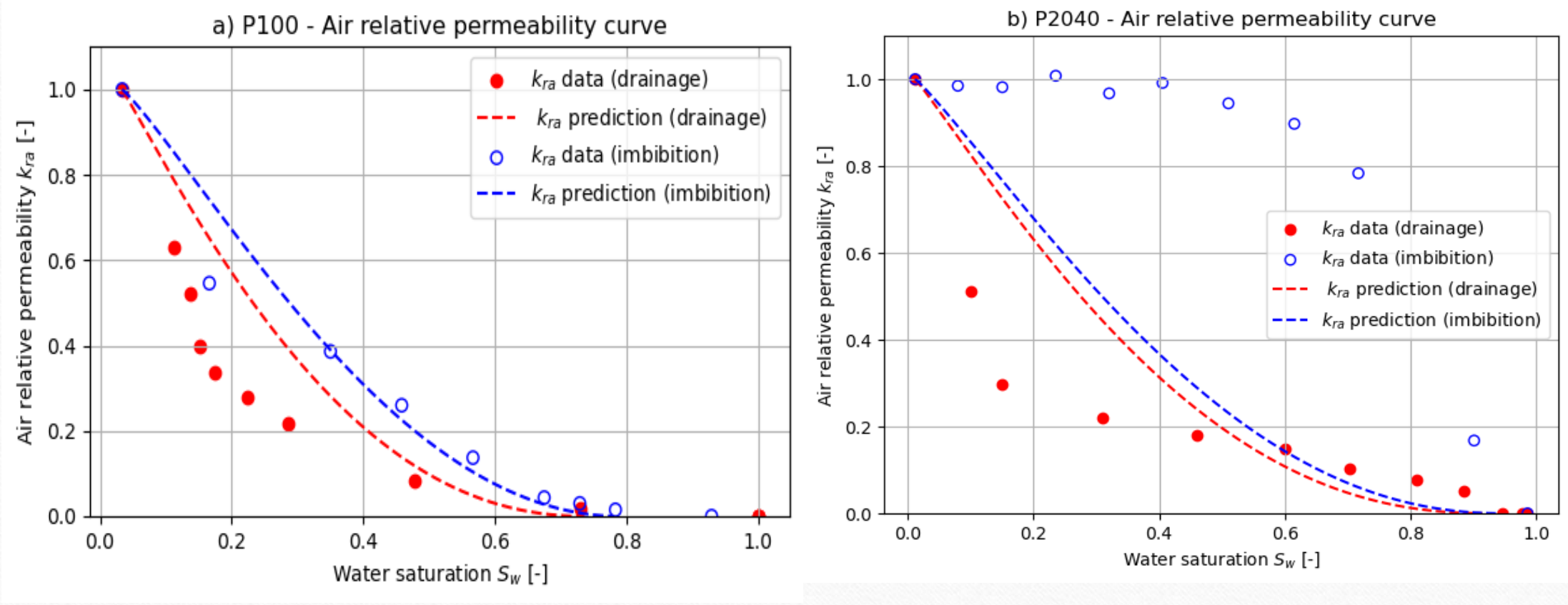

Fig. 13 Air relative permeability (kra) as function of water saturation (Sw) for sands P100 and P2040. Experimental data are shown for drainage (red filled circles) and imbibition (blue unfilled circles). Solid lines represent the predicted kra curves obtained from the van Genuchten model.

Ongoing work: OpenFOAM simulations

Pore-scale numerical modelling based on X-ray microtomography images is currently being conducted using OpenFOAM to investigate the microscopic displacement mechanisms observed experimentally.

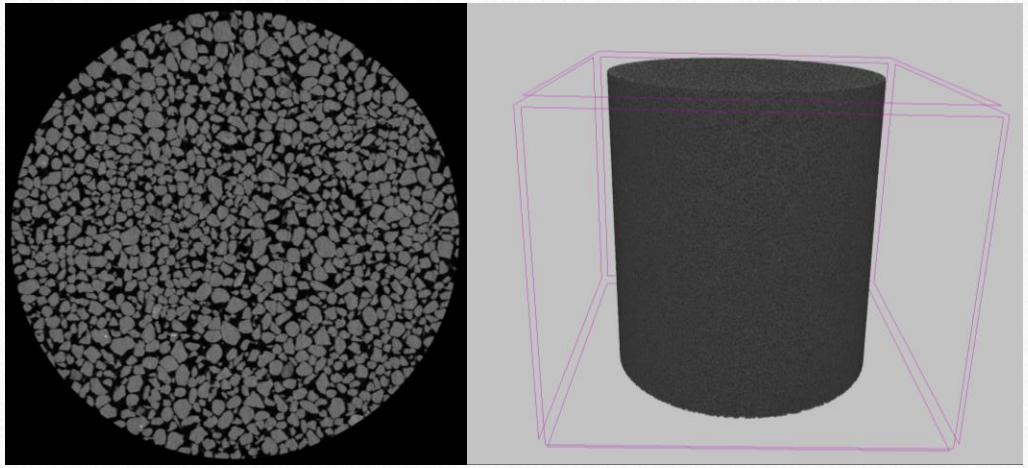

Fig. 14 X-ray tomography images and reconstruction for the coarse sand P2040.

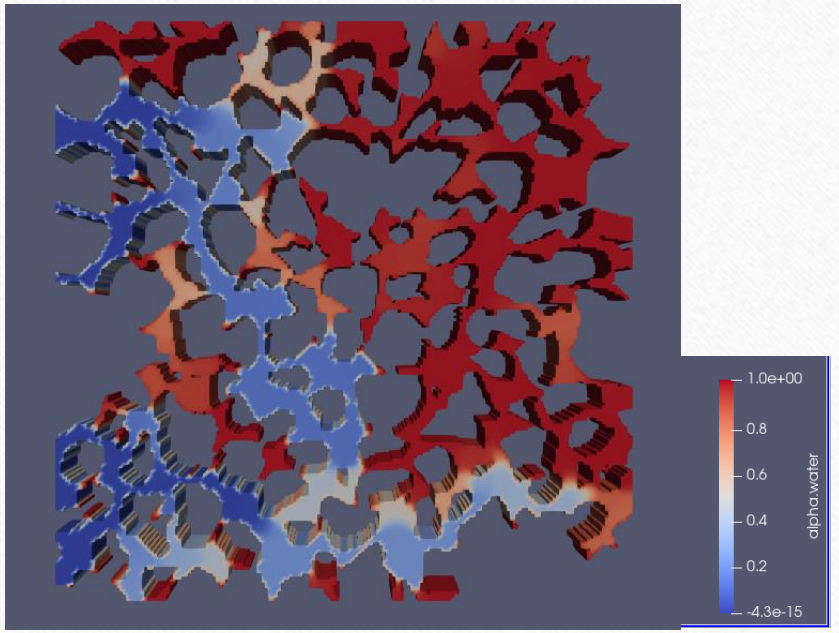

Fig. 15 Simulation of the drainage process during air injection.

Take-home messages

- Wettability strongly controls water retention and air–water relative permeability curves.
- Oil-wet and fractionally wet sands exhibit pronounced hysteresis in relative permeability curves.
- A plateau in k_{ra} was observed during imbibition in low-capillarity sands: possible contribution of viscous coupling?
- Existing mathematical models fail to reproduce most of the experimental relative permeability data.

Université de Strasbourg

Thank you!

Institut Terre & Environnement de Strasbourg | ITES | UMR 7063 de l'Université de Strasbourg & cnrs & ENGEES

Learn more

Gerhard Schäfer, Kevin Hernandez Perez, Panav Hulsurkar, Magda Ibrahim Youssif, François Lehmann, Mohammad Piri,
Influence of wettability on water retention curves in unconsolidated porous media,
Journal of Contaminant Hydrology, Volume 269, 2025.

Learn more

Kevin Hernandez-Perez; Gerhard Schäfer; François Lehmann; Mohammad Piri; Renaud Toussaint.
An innovative experimental device to quantify the water relative permeability and in situ water retention curves of unconsolidated porous media.
Comptes Rendus. Géoscience, Volume 357 (2025)

Learn more

Kevin HERNANDEZ-PEREZ, Gerhard SCHÄFER, Amir H. Alizadeh et al.
Design of a hydraulically confined column device for simultaneous measurement of air relative permeability and water retention in unconsolidated porous media, 28 April 2026, PREPRINT (Version 1)